

# Physics of Fluids at Low Reynolds Numbers—A Molecular Approach

Joel Koplik and  
Jayanth R. Banavar

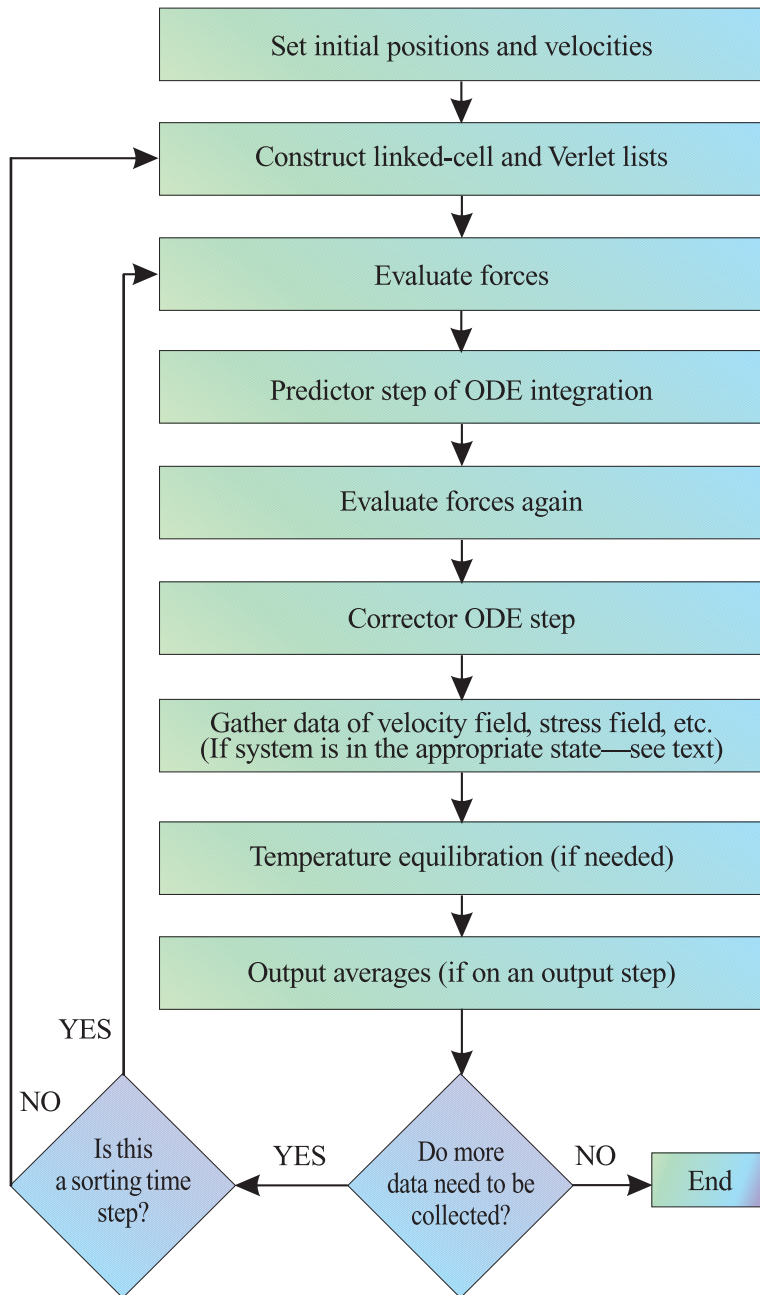


Figure 1. Sketch of computational algorithm for a molecular-dynamics simulation.

The advent of powerful computers and novel programming techniques has opened a new window on diverse problems in physics. Our focus, in this article, is on a set of issues pertaining to the behavior of fluids, at low Reynolds numbers, for which the inertial forces are tiny compared to viscous forces.

We shall discuss classes of long-standing problems for which a computational approach yields qualitatively new information that is inaccessible using conventional methods. Broadly speaking, these problems involve questions of behavior at the subcontinuum level for which experiments are unable to provide the requisite answers. In these cases, com-

puters provide a bridge between microscopic and macroscopic scales and are beginning to yield new insights into technologically important issues. The computational method is molecular-dynamics (MD) simulation, which entails the integration of Newton's laws of motion for a set of interacting molecules (see the flow diagram in Fig. 1).

At the simplest level, molecular simulations are important for the interpretation of nanoscale experiments. A detailed understanding of the behavior of materials at very small scales is necessary for the fabrication of miniature devices and the manipulation of materials at the molecular scale. The behavior of materials at the nanoscale is often quite different from that in the bulk. For example, it has been found recently that very small systems may exhibit solid-liquid coexistence over a range of temperatures, quite distinct from the macroscopic behavior described by equilibrium statistical mechanics.<sup>1</sup> Another example occurs in studies of friction in narrow systems,<sup>2</sup> in which a combination of experiment and simulation has elucidated the relationship between the stick-slip behavior observed in experiments and the local freezing and melting first discovered in MD simulations by Thompson and Robbins.<sup>3</sup>

Microscopic studies are needed to assess the range of

Joel Koplik is a professor at the Benjamin Levich Institute and Department of Physics, City College of New York, New York, NY 10031. E-mail: koplik@sci.cuny.cuny.edu  
Jayanth R. Banavar is a professor in the Department of Physics and Center for Materials Physics, 104 Davey Laboratory, The Pennsylvania State University, University Park, PA 16802. E-mail: jayanth@phys.psu.edu

validity of traditional continuum theories. Even the simplest liquids display anomalous behavior under high shear rates,<sup>4</sup> at sharp corners in flow domains,<sup>5</sup> or in the presence of interfacial contaminants.<sup>6</sup> Computer simulation can explore regimes for which well-controlled, high-resolution experiments are difficult. More important, molecular-scale investigations are vital for bridging the scales and allow for the construction of hybrid models in which a crucial subsystem is treated with atomic-scale resolution and embedded in a continuum that is treated with traditional methods.<sup>7</sup>

Atomistic simulations are an invaluable tool for deducing constitutive relationships, which may then be fed into continuum calculations. The deduction of boundary conditions from first principles is an obvious example, but for fluid flow in any non-Newtonian regime there is no consensus on the correct rheological model.<sup>8</sup> In nanodevices, for example, one immediate problem is that deviations from Navier-Stokes behavior occur in very narrow channels,<sup>9</sup> but beyond this regime researchers must consider such effects as surface interactions and the flexibility of thin solids.<sup>10,11</sup> When there is any doubt about the correct averaged description, it is appropriate to study the dynamics at a finer scale of resolution, that of the atomic constituents.

The subcontinuum fluid problems that have been studied by molecular simulations include:

- situations in which continuum fluid mechanics is inapplicable, for example, the rupture or coalescence of liquid drops that occur on interfacial scales quite disparate from bulk continuum length or time scales;<sup>12-14</sup>
- unphysical singularities that result from an application of continuum approach-

es, for example, corner-flow singularities,<sup>15,16</sup> the Stokes drag on an object falling in a fluid as it approaches a solid surface,<sup>17</sup> and the divergence of the dissipated energy when one fluid pushes another past a solid surface due to a breakdown of no-slip boundary conditions in the vicinity of the moving contact line;<sup>18-20</sup>

- interfacial phenomena entailing thin liquid films for which the continuum approximation is not valid and the substrate-fluid interaction plays a crucial role, as in the dynamics of spreading of wetting films on solid surfaces<sup>21-23</sup> and freezing in confined geometries;<sup>24-27</sup>
- the behavior of non-Newtonian fluids<sup>16</sup> for which the constitutive relationships are often unknown and the governing equations are nonlinear, rendering analytic analysis difficult.

A powerful strategy is to construct a very-small-scale version of the experiment on the computer with dimensionless operating conditions (such as Reynolds number) in the regime of interest and then focus on the appropriate local or bulk features. The key fact that makes such a procedure viable is that the continuum description applies even when the linear size of the system is minuscule and accommodates  $O(10)$  molecules.<sup>28</sup>

A typical MD computer simulation<sup>29-31</sup> begins with a set of molecules occupying a region of space in three dimensions. Each molecule is assigned a random velocity corresponding to a Boltzmann distribution at the temperature of interest. The interaction of the

*Digital  
simulations  
are yielding  
new information on  
the behavior  
of viscous  
flows.*

molecules is prescribed in the form of a potential energy, and the time evolution of the molecular positions is obtained by integrating Newton's equations of motion. The calculation keeps track of all molecular positions and velocities as a function of time, and from this the instantaneous configuration of the system can be examined. In addition, appropriate averages are computed if the system is in the state of interest—for example, in equilibrium, steady state, or state of dynamical evolution (denoted as an “appropriate state” in Fig. 1).

The Eulerian velocity at a particular point and time is computed approximately as a time average of the particle velocities of the molecules occupying a sampling bin about the point over some time interval. Likewise, the local temperature is the average kinetic energy in a bin, and the stress tensor is the average of an appropriate expression involving molecular momentum and forces (due to Irving and Kirkwood).<sup>54</sup> The latter quantities may then be directly compared with experiment and the predictions of the continuum equations.

Because an MD calculation operates at very fine spatial and temporal resolution, there are limitations on the size and duration of a simulated system. Typical calculations involve nanometer-sized regions and time intervals of nanoseconds. The largest simulations currently possible can exceed these limits only by a factor of 10 or perhaps 100, and so they intrinsically treat a microscopic system. Although a molecular simulation with valid interatomic potentials can undoubtedly produce the correct dynamics for a system of just that number of atoms, the key issue in applying the results to bulk behavior is whether the simulated sample is large enough to represent a continuum faithfully. In the case of simple molecules that correspond to Newtonian fluids, the evidence is quite positive.<sup>28</sup> A rule of thumb obtained from the comparison between simulation and experiment is that continuum behavior sets in when the system size is about 10 molecules per fluid species per direction of space.

For neutral, polarizable, spherically symmetric molecules, such as liquid argon, the Lennard-Jones potential

$$V_{LJ}(r) = 4\epsilon \left[ \left( \frac{r}{\sigma} \right)^{-12} - \left( \frac{r}{\sigma} \right)^{-6} \right]$$

between two atoms separated by distance  $r$  is quantitatively accurate. The parameters  $\epsilon$  and  $\sigma$  provide the scales of energy and distance, and the mass scale  $m$  is taken to be that of the molecules composing the fluid. The resulting natural time step is the period of oscillation about the potential minimum,  $\tau = (m/\epsilon)^{1/2}$ . For liquid argon, the characteristic time scale is  $\tau = 2.2 \times 10^{-12}$  s. To simulate the flow of a Newtonian fluid within passive boundaries, this potential is sufficient, because any differences are manifested in transport coefficients, which are lumped into dimensionless operating parameters such as the Reynolds number.

In more general cases, or if surface interactions are significant, the molecular structure must be specified in more detail. The interaction potential for polymer chains may be chosen to have two parts—a potential that exists between all the monomers and a strongly attractive part that acts only

between crosslinked monomers or monomers along the sequence of the chain.<sup>32</sup> A common choice for the latter is the finitely extensible nonlinear elastic (FENE) potential

$$V_{FENE}(r) = \frac{k}{2} \log \left( 1 - \frac{r^2}{r_0^2} \right)$$

and the properties of the resulting model polymer melt have been obtained in detail by MD simulations.<sup>33</sup>

The FENE model is designed to produce a non-Newtonian fluid that is tractable for computer simulations but does not necessarily quantitatively reproduce the properties of any specific polymer liquid. This is analogous to the use of a truncated Lennard-Jones potential for simulations of a Newtonian liquid. Although the resulting “computer fluid” has properties similar to liquid argon, there are distinct numerical differences in its behavior, which are irrelevant once the results are exhibited in terms of variables that have been rendered nondimensional in terms of the material properties of this liquid. The FENE model can be regarded as either a coarse-grained description or a microscopic description of some idealized chain of actual monomers, but it has been demonstrated by simulation to have the appropriate properties of shear-thinning, normal stress differences, and conformational changes under shear.<sup>4,33,34</sup>

In order for the fluid-solid interaction to be captured correctly, it is necessary to treat solid walls at the same resolution as the fluid, since their constituent sizes are comparable. The simplest semirealistic wall has solid atoms that are attached to lattice sites by a confining potential and interact with the fluid through a Lennard-Jones potential.<sup>19</sup> In this way the solid and fluid atoms realistically exchange energy, and the action of a laboratory thermostat can be imitated by controlling the temperature of the outer parts of the walls not in direct contact with the fluid.

Viscous flows generate heat, which can significantly raise the temperature of a small system. When the actual system of interest is microscopic, the heating is realistic; otherwise, it is an artifact that must be corrected. The easiest method of temperature control is constant-kinetic-energy equilibration, in which the velocity of each molecule is rescaled at regular intervals, but this is rather unphysical. For homogeneous systems, at least, the equations of motion can be altered to couple the molecules to a thermostat.

Nosé and Hoover<sup>35</sup> have shown that by including an additional degree of freedom that represents a reservoir characterized by some thermal inertia and employing appropriate equations of motion, researchers may generate configurations belonging to either the canonical or the constant-temperature/constant-pressure ensemble. Another alternative, if the simulation involves a solid boundary, is to extract heat from the outer parts of the boundary, in imitation of the cooling of the apparatus in a laboratory. Although the standard MD method employs the microcanonical ensemble (fixed energy, volume, and number of particles), considerable progress has been made in developing ensembles that resemble the conditions (such as constant pressure) often encountered in experiments.<sup>30</sup>

The computation itself is the integration of a large set of coupled ordinary differential equations (ODEs) for molecular positions; the driving terms of these equations represent the force of one molecule due to the others. ODE algorithms lend themselves to vectorization or parallelization easily, and so the bulk of the computation is the force calculation.

If the force is long-ranged, the program must sum over all pairs at each step, and computation times are necessarily  $O(N^2)$ . For short-range forces, the computation time can be reduced if the pairs of interacting atoms are kept track of via a "Verlet list." In its simplest form, this method stores for each atom a list of those atoms within a sphere whose radius is the interaction range plus a small "skin" thickness. The latter, and the integration time step, are chosen so that for a time interval of  $S$  (typically 10 to 20 steps) no atoms outside the skin are likely to enter the interaction range. After each such interval, the list must be recomputed (in a time step that is denoted as a sorting time step in Fig. 1), and the result is a computation time  $O(N) + S^{-1} \cdot O(N^2)$ .

A strictly  $O(N)$  computation can be achieved by a linked-cell list, which divides the physical volume into smaller cells such that each molecule within a subcell interacts at most with molecules in its own subcell and the neighboring subcells. Some overhead is associated with the cells, so that the simple Verlet method is faster for smaller systems, but for a large number of particles, a combination of a Verlet table, a link-cell algorithm, and a layering algorithm<sup>36</sup> is effective.

We have recently developed a parallel code based on platform-independent Message Passing Interface (MPI) routines.<sup>37</sup> The code consists of a layered linked-cell list and a domain decomposition of the configuration space of the simulation. The latter is divided into link cells of size slightly larger than the interaction range.

The three-dimensional configuration space is mapped onto a two-dimensional grid of processors, so that each processor is responsible for particles within a parallelepiped formed by a vertical column of cells. The force calculation for a given cell uses coordinates of particles within its own domain, plus particle information from neighboring cells belonging to other processors. The latter is communicated to each cell by MPI calls and stored in a buffer area.

Each processor calculates the forces arising between its own particles, and between its particles and those in the buffer area. To complete the time step, the forces on the buffer particles are sent by MPI back to their respective processors, and particle positions and velocities are advanced using the ODE algorithm. The code performance is on the order of one CPU second per time step on a Cray T3E for million-atom simulations.

We turn now to a few applications. We refer the reader to an earlier review on continuum deductions from molecular hydrodynamics<sup>28</sup> and a more recent one on molecular simulations of viscous flows<sup>20</sup> for other examples. In the applications discussed below, the number of molecules was typically of the order of tens of thousands and the number of integration time steps of the order of hundreds of thousands. In situations corresponding to steady-state flows, long runs can be carried out to improve the signal-to-noise ratio. This is further facilitated in geometries in which there is translational invariance

along one of the directions, allowing for additional spatial averaging.

The coalescence of two drops of a liquid (or the inverse problem of the rupture of a body of liquid into two parts) is, on the whole, a problem of continuum fluid mechanics, but the fine structure of the process and the rearrangements of the interfacial boundaries occur at the molecular scale. Several of our calculations have examined the rupture and coalescence of immiscible fluid interfaces. The simplest case that can be considered as an example of rupture is the Rayleigh instability of a liquid cylinder in vapor. The gross behavior agrees with hydrodynamics, even though shape and thermal fluctuations result in local velocity and stress fields that are so noisy as to be unresolvable.

More controlled calculations involved drops of one liquid surrounded by an immiscible background fluid, undergoing either linear shear or plane-extensional flow generated by solid boundary motion. In this case, we have found rather good agreement between the dynamics of microscopic (30-Å) drops and laboratory experiment and continuum calculations.<sup>12</sup> Similar calculations have studied the coalescence of two drops in a background shear and the merger of a drop with a bath of fluid.<sup>13</sup>

Although the local fields are still too noisy to quantify in these calculations, and it is therefore not possible to extract a boundary condition for interface rupture, the microscopic mechanism in this process may be identified as one of "tendrils breaking." Molecules from a drop will occasionally thermally fluctuate away from the bulk, and when two drops are nearby, the fluctuating molecules of one drop may come within the interaction range of those of the other. These molecules are then drawn together, and in the process they draw along molecules from their respective bulk drops, forming a tendril of mutually attracting molecules. The result is a dumbbell shape, which surface tension contracts into a sphere by thickening the tendril.

Motivated by experiments by Dell'Aversana and collaborators,<sup>38</sup> we then studied the *non*-coalescence of drops when there is relative motion between them. Macroscopically, a shear flow or temperature gradient can entrain a moving air film between two liquid bodies, which produces a lubrication force resisting their van der Waals attraction. Microscopically,<sup>14</sup> the fluid motion causes a drop to rotate, and this rotation breaks the joining tendril before it can thicken and cause the drops to merge.

As an illustration of this class of calculations, we show some coalescence simulations. Figure 2a depicts the coalescence of a cylinder of liquid with a bath of fluid. The cylinder, with a radius of  $6\sigma$  and length  $26\sigma$ , is made up of 2235 molecules and falls under the influence of gravity of strength  $0.3\sigma/\tau^2$  into a tank of 4500 molecules of the same liquid in the presence of an immiscible background fluid (not shown) and a solid plate in the bottom. The falling cylinder displaces the background fluid during its downward motion and causes a distortion of the bath surface. The initial contact is in the form of a localized filament. As the cylinder approaches the bath, the filament thickens, and the coalesced region moves outward from the point of first contact, zippering the two bodies of fluid together. This qualitative picture is also seen

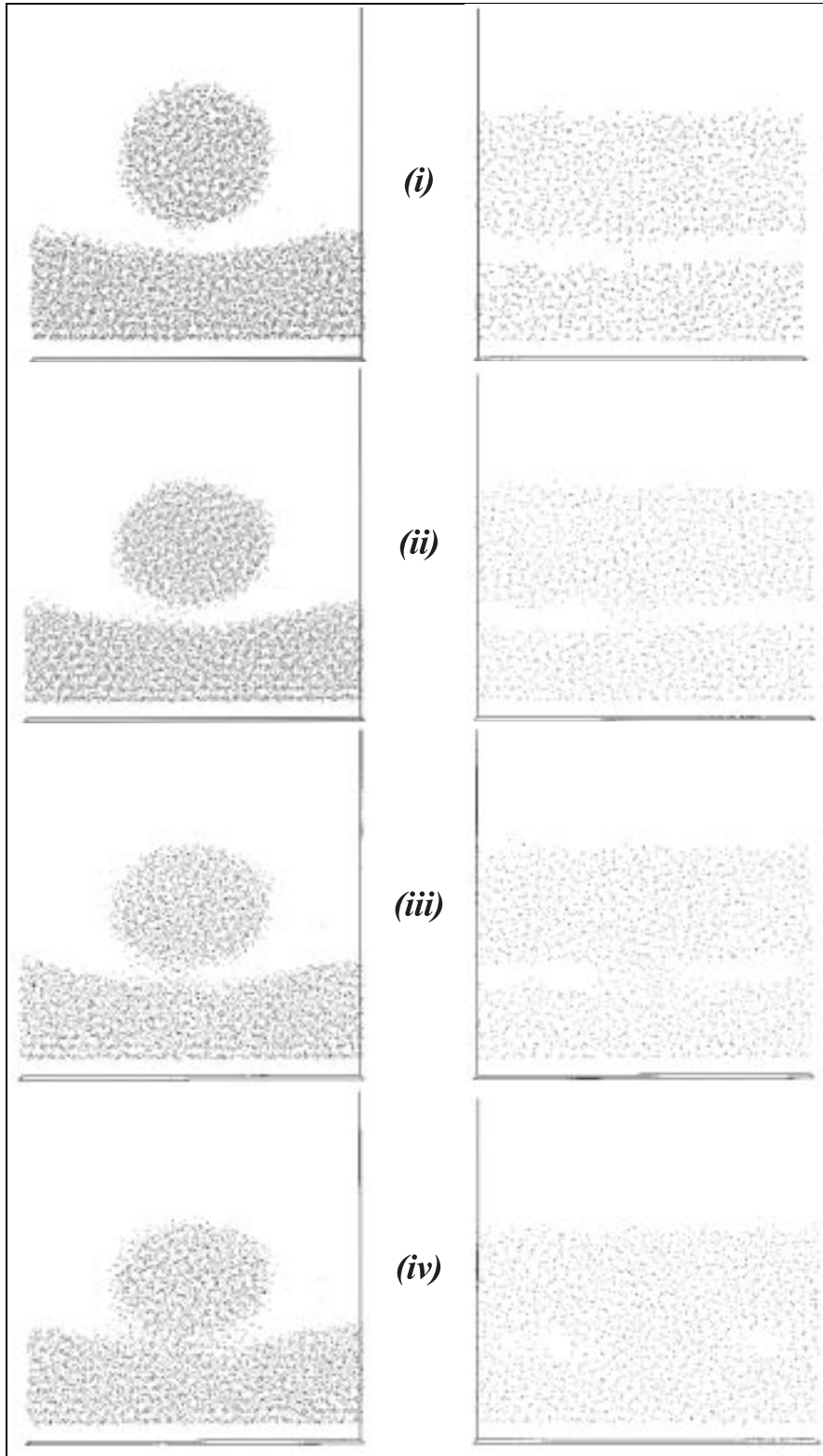


Figure 2a. Fall of a liquid cylinder into a bath under gravity, through an immiscible background fluid, which is not displayed. Times shown are (i)  $40\tau$ , (ii)  $42.5\tau$ , (iii)  $45\tau$ , and (iv)  $50\tau$ . Side view on right represent a vertical section of width  $5.65\sigma$  parallel to the axis of the cylinder.

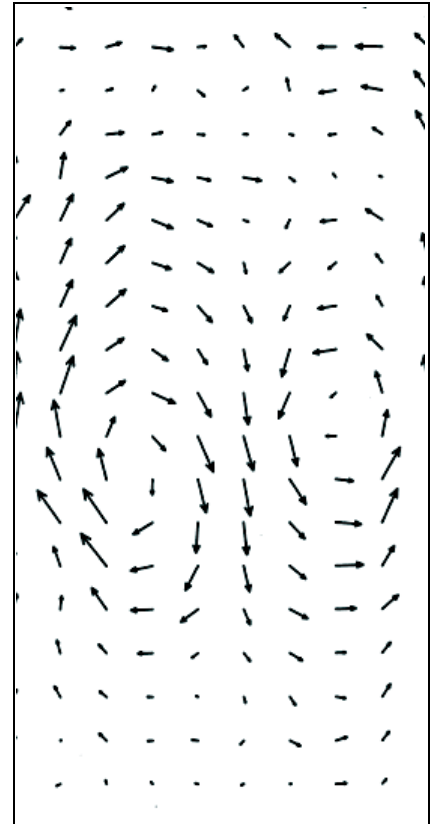


Figure 2b. Flow field corresponding to fig. 2a: velocity components in the plane perpendicular to the cylinder axis, averaged over the time interval  $60\tau \leq t \leq 62.5\tau$  after the merger has occurred. The largest arrow shown corresponds to velocity  $4.0 (\sigma/\tau)$ .

The Eulerian velocity field is obtained by accumulating the average molecular velocities in a fixed array of sampling bins, averaged over the direction of the cylinder axis. The result (see Fig. 2b) shows the expected dipole vortex flow as the cylinder displaces the bath fluid. At earlier and later times, the velocity field indicates the drop descending and the bath fluid splashing upward, respectively. The stress tensor is, unfortunately, too sensitive to thermal fluctuations for it to be reliably evaluated as part of these calculations.

### The physics of wetting

The spreading of liquids on solid surfaces is a familiar but an incompletely understood phenomenon, with major implications both in daily life and in diverse technologies including oil recovery,<sup>39,40</sup> painting,<sup>41</sup> and film and spray coating.<sup>42</sup> The degree to which a particular liquid “wets” its bounding surface controls how it can be processed

in other cylinder-coalescence events, including a four-roller flow in which the merger is mainly driven by surface tension.

and spray coating.<sup>42</sup> The degree to which a particular liquid “wets” its bounding surface controls how it can be processed

and dictates many of its uses. The basic microscopic consideration is the preferential attraction of a surface for one fluid phase compared to another and entails the interatomic forces as well as the structure and possible heterogeneities of the materials. Furthermore, a three-phase contact region provides a rich array of physical questions.<sup>43-45</sup>

Earlier MD calculations have studied static meniscus shapes<sup>46</sup> and the contact-line-singularity question,<sup>18,19</sup> and we have begun to consider hysteretic effects.<sup>47</sup> Although the interfacial region is intrinsically microscopic and thus well-suited for molecular calculation, the time scales for interfacial problems can be macroscopic. Simulations of wetting are thus on the edge of feasibility due to computer-time limitations, and many opportunities for new results and methodologies exist.

We and others<sup>21-23</sup> have addressed the origin of the unusual "terraced spreading" observed experimentally by Heslot *et al.*,<sup>48</sup> a variant form of complete wetting in which certain polymeric liquids spread in the form of pronounced monomolecular layers. Our initial simulations<sup>21</sup> using Lennard-Jones atoms and dumbbell molecules showed that layering resulted from a strong fluid-solid attraction coupled to excluded-volume constraints. However, the simulated growth rate was subdiffusive and slower than that seen experimentally. At the time, we conjectured that the discrepancy was due to the small size of the molecules involved, and we began a new set of simulations<sup>23</sup> using chains of length 8 and 16 (see Fig. 3). In these new simulations the larger molecules do indeed spread at the experimentally correct rate. The origin of the difference is that small molecules can easily be pinned at minima of the solid-fluid interaction potential, whereas the pinning of larger molecules is less effective because the bond length in the molecules is incommensurate with the atomic spacing in the solid lattice.

### Non-Newtonian fluids

A non-Newtonian fluid is characterized by an internal structure that is sensitive to its dynamic environment and whose structural changes under flow conditions feed back and alter the flow. Often such fluids are polymer so-

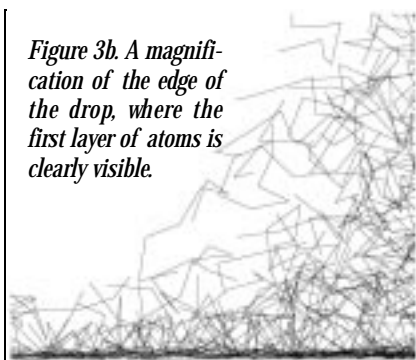


Figure 3b. A magnification of the edge of the drop, where the first layer of atoms is clearly visible.

lutions or melts, in which the stress produced by the flow changes the molecular configuration of the polymer chains. The flow properties of non-Newtonian fluids have received increasing attention<sup>49,50</sup> as the technological applications of these materials blossom. On the continuum scale, the changes in microstructure under flow render the Navier-Stokes equations inappropriate for non-Newtonian fluids, and considerable effort has been devoted to viscometric experiments<sup>51</sup> and the development of realistic constitutive relationships.<sup>8</sup> It is difficult to treat the dynamics of complicated molecules theoretically in realistic detail, and a considerable literature exists on various approximate methods and phenomenological equations of motion.

From the molecular point of view, a Newtonian fluid such as the Lennard-Jones liquid is characterized by a single time scale that is short compared to the characteristic times associated with practical flows. The internal time scale may be taken as the period of oscillations about the potential minimum, realistically in the picosecond range, and only under unusual circumstances does an applied frequency or imposed strain rate approach such values. In such conditions, which we have previously considered in "singular" situations such as the moving-contact-line<sup>18</sup> and sliding-plate<sup>15</sup> problems, the fluid cannot relax its internal structure before its environment changes, and viscoelastic effects appear.

Non-Newtonian behavior most commonly occurs when the fluid has a wide range of internal time scales, extending up into the operating range of the flow in question. A common microscopic model that exhibits this behavior is a chain of atoms linked by the FENE potential mentioned earlier, in which the structure ranges from coiled to extended and varies under applied hydrodynamic fields. Aside from incorporating the relevant physical mechanism, this model has the advantages of (relative) computational simplicity and a known rheological behavior, as determined by earlier MD simulations.<sup>33</sup>

Although a range of non-Newtonian behavior is found for chains of any length, and new quantitative results for non-Newtonian flows have been obtained for lengths of 10–30 atoms,<sup>16,52</sup> simulations of long chains are particularly desirable so as to allow for the possibility of chain entanglements.

A recent study focused on the nature of the reentrant corner-stress singularity (see Fig. 4). All fluids show some divergence in the shear stress in flow past a reentrant (contracting) corner due to an assumption of the no-slip boundary condition in continuum calculations. Realistically, of course, there is no physical divergence because the governing continuum equations apply only above some microscopic length

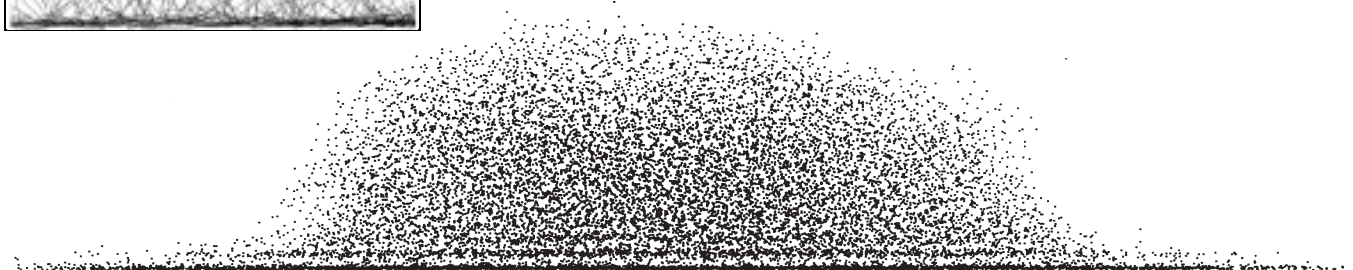
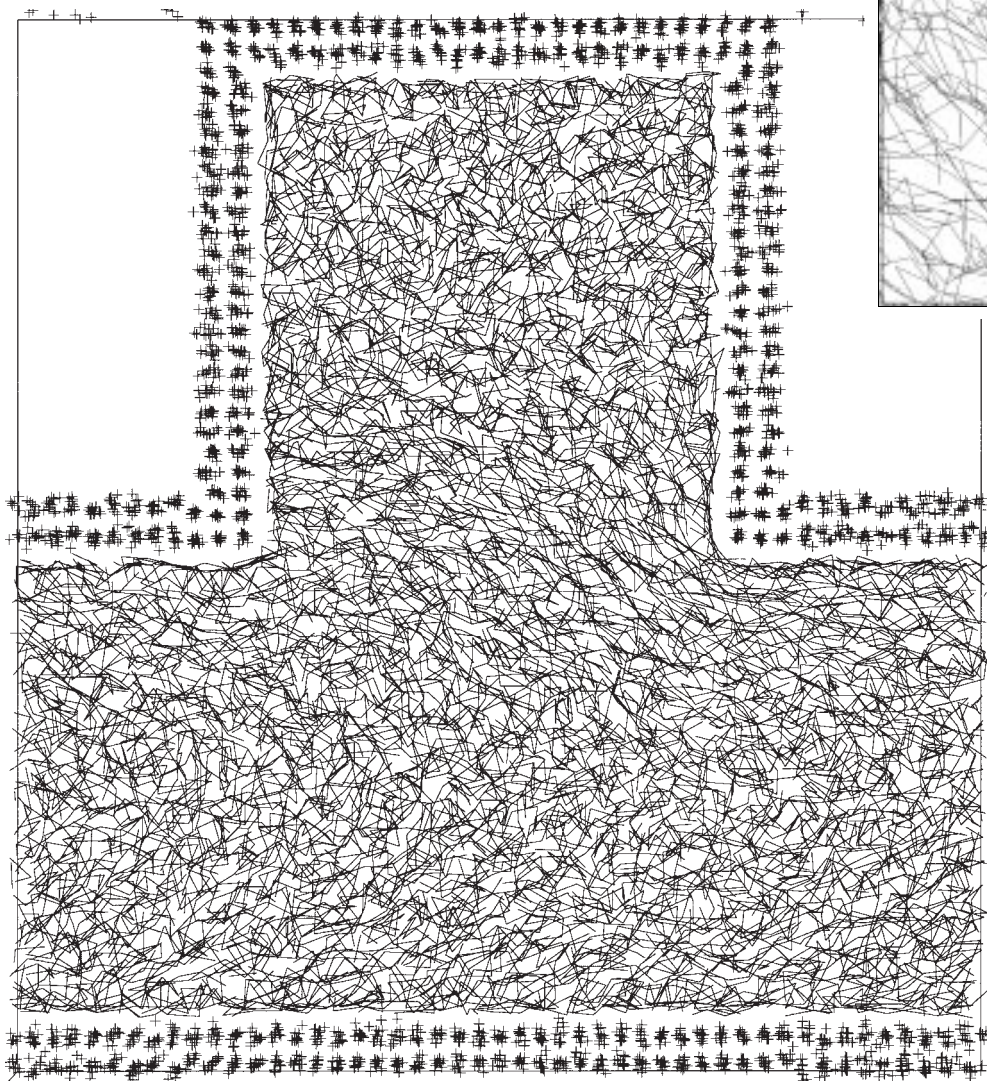


Figure 3a. A drop of 2048 8-atom molecules during spreading.



*Figure 4a. Snapshot of an instantaneous molecular configuration of a liquid made up of 10-atom molecules during flow in a channel of two widths under constant acceleration to the right, in projected view. The molecular bonds are shown as lines and the wall atoms, as plus signs.*

scale comparable to a molecular size, and at very short distances the fluid motion is governed by smoothly varying interatomic potentials. The exponent characterizing the power-law divergence is known for simple Newtonian fluids but is a subject of controversy in the non-Newtonian case.<sup>5</sup> We carried out simulations of the flow of both types of fluid through an atomistic channel with a reentrant corner; in the Newtonian case we reproduced the analytic result of Moffatt,<sup>53</sup> whereas for FENE fluids we found a systematically higher stress exponent.<sup>16</sup> The physical mechanism is that the flow elongates chain molecules near a corner and enhances the stress thereby.

### **Simulations complement experiments, theory**

Molecular-dynamics simulations of fluids have become an effective complement to experiments and continuum theory. In dynamical situations, for which there is no steady state, and hence time-averaging to improve the signal-to-noise ratio is not feasible, the simulations are at present only partially able to approximate continuum behavior: average quantities such as shapes may be studied in detail, but the Navier-Stokes

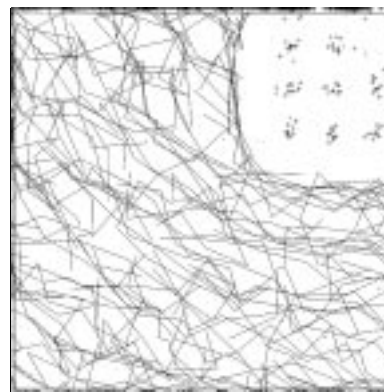


*Figure 4b. Blow-up of the reentrant corner.*

fields are often too noisy to resolve. This highlights an outstanding problem in molecular dynamics, as well as in some other calculational techniques: how to match regions that are to be treated at different scales of resolution. In the case of multigrid methods for the finite-difference solution of differential equations, for example, the problem is relatively benign, because the same sort of equation is solved at all resolutions and the issue is one of interpolating between a coarse scale and a fine one. In the present case, researchers would like to match a molecular simulation of, say, the neck of a rupturing liquid thread to a Stokes equation describing the bulk liquid away from the neck. The difficulty is that the variables of the calculation in the two regions are entirely different. Molecular velocities and positions must be chosen

to correspond to a specified average velocity and stress tensor, which in turn may vary weakly in space and time. There have been a few recent promising developments<sup>7</sup> in the matching problem, but so far these have been restricted to test cases. We look forward to an assessment of the robustness of these matching schemes and further applications leading to new physics.

Molecular-dynamics simulations have provided conceptual and quantitative results on the origin and limitation of boundary conditions, the behavior of fluid interfaces under rupture and coalescence, the local dynamics of lubrication and wetting films, and the rheology and flows of complex fluids. An improvement of two orders of magnitude in computational power would be sufficient to resolve many of the unresolved questions and allow for the direct extraction of continuum boundary conditions.

### **Acknowledgments**

We are indebted to our collaborators for their participation in this research, and to NASA and the National Science Foundation for financial support.

## References

1. S. Sugano, *Microcluster Physics* (Springer, Berlin, 1991).
2. B. Bhushan, J. N. Israelachvili, and U. Landman, *Nature* **374**, 607 (1995).
3. P. A. Thompson and M. O. Robbins, *Science* **250**, 792 (1990).
4. W. Loose and S. Hess, *Rheol. Acta* **28**, 91 (1989).
5. See, for example, the following consecutive group of papers in *J. Non-Newtonian Fluid Mech.* **50**: M. Renardy, 127–134; R. I. Tanner and X. Huang, 135–160; E. J. Hinch, 161–172; and A. R. Davies and J. Devlin, 173–192 (1993).
6. R. F. Probst, *Physicochemical Hydrodynamics*, 2nd ed. (Wiley, New York, 1994).
7. S. T. O'Connell and P. A. Thompson, *Phys. Rev. E* **52**, R5792 (1995); N. G. Hadjiconstantinou and A. T. Patera, *Int. J. Mod. Phys. C*, **8**, 967 (1997).
8. R. G. Larson, *Constitutive Equations for Polymer Melts and Solutions* (Butterworths, Boston, MA, 1988).
9. I. Bitsanis *et al.*, *J. Chem. Phys.* **89**, 3252 (1988); K. P. Travis, B. D. Todd, and D. J. Evans, *Phys. Rev. E* **55**, 4288 (1997).
10. R. E. Tuzun *et al.*, *Nanotechnology* **7**, 241 (1996).
11. J. Gao, W. D. Luedtke, and U. Landman, *Science* **270**, 605 (1995).
12. J. Koplik and J. R. Banavar, *Phys. Fluids A* **5**, 521 (1993).
13. J. Koplik and J. R. Banavar, *Science* **257**, 1664 (1992).
14. P. Dell'Aversana, J. R. Banavar, and J. Koplik, *Phys. Fluids A* **8**, 15 (1996).
15. J. Koplik and J. R. Banavar, *Phys. Fluids A* **7**, 3118 (1995).
16. J. Koplik and J. R. Banavar, *Phys. Rev. Lett.* **78**, 2116 (1997); *J. Rheol.* **41**, 787 (1997).
17. M. Vergeles *et al.*, *Phys. Rev. Lett.* **75**, 232 (1995); *Phys. Rev. E* **53**, 4852 (1996).
18. J. Koplik, J. R. Banavar, and J. F. Willemsen, *Phys. Rev. Lett.* **60**, 1282 (1988); *Phys. Fluids A* **1**, 789 (1989).
19. P. A. Thompson and M. O. Robbins, *Phys. Rev. Lett.* **63**, 766 (1989); P. A. Thompson, W. B. Brinckerhoff, and M. O. Robbins, *J. Adhesion Sci. Technol.* **7**, 535 (1993).
20. J. Koplik and J. R. Banavar, "Molecular Dynamics of Viscous Flow," *JSME Int. J.* **41**, 353 (1998).
21. J.-x. Yang, J. Koplik, and J. R. Banavar, *Phys. Rev. Lett.* **67**, 3539 (1991); *Phys. Rev. A* **46**, 7738 (1992).
22. J. Nieminen *et al.*, *Phys. Rev. Lett.* **69**, 124 (1992); J. Nieminen and T. Ala-Nissila, *Phys. Rev. E* **49**, 4228 (1994).
23. J. De Coninck *et al.*, *Phys. Rev. Lett.* **74**, 928 (1995); *Phys. Rev. E* **53**, 562 (1996).
24. D. D. Awschalom and M. W. Schafer, *Phys. Rev. Lett.* **57**, 1753 (1986); J. N. Israelachvili, P. M. McGuiggan, and A. M. Homola, *Science* **240**, 189 (1988); M. L. Gee *et al.*, *J. Chem. Phys.* **93**, 1895 (1990); B. S. Schirato *et al.*, *Science* **267**, 369 (1995).
25. W. J. Ma, J. R. Banavar, and J. Koplik, *J. Chem. Phys.* **97**, 485 (1992).
26. P. E. Sokol *et al.*, *Appl. Phys. Lett.* **61**, 777 (1992).
27. W. J. Ma *et al.*, *Phys. Rev. E* **51**, 441 (1995).
28. J. Koplik and J. R. Banavar, *Annu. Rev. Fluid Mech.* **27**, 257 (1995).
29. F. F. Abraham, *Adv. Phys.* **35**, 1 (1986).
30. M. P. Allen and D. J. Tildesley, *Computer Simulation of Liquids* (Clarendon Press, Oxford, England, 1987).
31. G. Ciccotti and W. G. Hoover (editors), *Molecular Dynamics Simulations of Statistical Mechanical Systems* (North Holland, Amsterdam, 1986).
32. R. B. Bird *et al.*, *Dynamics of Polymeric Liquids*, 2nd ed. (Wiley, New York, 1987), Vol. 2.
33. M. Kröger, W. Loose, and S. Hess, *J. Rheol.* **37**, 1057 (1993).
34. K. Kremer and G. S. Grest, *J. Chem. Phys.* **92**, 5057 (1990).
35. S. Nosé, *Mol. Phys.* **52**, 255–268 (1984); W. G. Hoover, *Phys. Rev. A* **31**, 1695 (1985).
36. G. S. Grest, B. Dünweg, and K. Kremer, *Comput. Phys. Comm.* **55**, 269 (1989).
37. S. Pal, J. Koplik, and J. R. Banavar (unpublished).
38. R. Monti and P. Dell'Aversana, "Microgravity experimentation in non-coalescing systems," *Micrograv. Quart.* (1995); P. Dell'Aversana and G. P. Neitzel, *Phys. Today* **51**(1), 38 (1998).
39. W. G. Anderson, in *J. Pet. Tech.*: **38**, 1125 (1986); **38**, 1246 (1986); **38**, 1371 (1986); and **39**, 1453 (1987).
40. J. J. Tabor, in *Surface Phenomena in Enhanced Oil Recovery*, edited by D. O. Shah (Plenum, New York, 1981), pp. 13–52.
41. T. F. Tadros, in *Wetting, Spreading and Adhesion*, edited by J. F. Padday (Academic Press, New York, 1978), pp. 423–438.
42. G. F. Teletzke, H. T. Davis, and L. E. Scriven, *Chem. Eng. Comm.* **55**, 41 (1987).
43. E. B. Dussan V, *Annu. Rev. Fluid Mech.* **11**, 371 (1979); E. B. Dussan V, S. Garoff, and E. Ramé, *J. Fluid Mech.* **230**, 97 (1991); J. A. Marsh, S. Garoff, and E. B. Dussan V, *Phys. Rev. Lett.* **70**, 2778 (1993).
44. P. G. de Gennes, *Rev. Mod. Phys.* **57**, 827 (1985).
45. J. F. Joanny and L. Leger, *Rept. Prog. Phys.* **55**, 431 (1992).
46. J. Hautman and M. L. Klein, *Phys. Rev. Lett.* **67**, 1763 (1991), and earlier references therein.
47. W. Jin, J. Koplik, and J. R. Banavar, *Phys. Rev. Lett.* **78**, 1520 (1997).
48. F. Heslot, N. Fraysse, and A. M. Cazabat, *Nature* **338**, 640 (1989).
49. R. B. Bird, R. C. Armstrong, and O. Hassager, *Dynamics of Polymeric Liquids*, 2nd ed. (Wiley, New York, 1987), Vol. 1.
50. R. I. Tanner, *Engineering Rheology* (Clarendon Press, Oxford, England, 1988).
51. K. Walters, *Rheometry* (Halsted/Wiley, New York, 1975).
52. K. Binder, *Monte Carlo and Molecular Dynamics Simulation of Polymer Systems* (Oxford, New York, 1995).
53. H. K. Moffatt, *J. Fluid Mech.* **18**, 1 (1964).
54. J. H. Irving and J. G. Kirkwood, *J. Chem. Phys.* **18**, 817 (1950).